International Journal of Software & Hardware Research in Engineering (IJSHRE)
ISSN: 2347-4890 | ijournals.in/ijshre
Volume 14 Issue 10, October 2026

Simulation-Based Optimization of 3D-Printed PLA Octet-Truss Lattices Reinforced with Directionally Aligned Recycled Steel Fibers Using ANSYS

Gautam Agarwal[1], Nikunj Parikh[2]

Affiliation: Student, Center Point School, Nagpur[1]; Mentor, Own My Own Technology, Mumbai[2]

https://doi.org/10.26821/ijshre.14.10.2026.141002

ABSTRACT

Developments in 3D printing enable complex lattice structures to be formed that are otherwise challenging, if not completely impossible, to make using other techniques. There are multiple variations of lattice structures, but one of the more popular variations is the octet-truss lattice. While somewhat load-bearing, PLA, the most common material used in FDM, lacks sufficient strength. This study aims to assess the advantages of using recycled steel fiber reinforcement to improve the performance and load-bearing capacity of the lattice structures with little to no incorporation of additional experimentation and sample fabrication. The sample was created and modeled in CAD, and then imported to ANSYS. The sample was then homogenized and low-steel fiber loadings (0.5%, 1%, and 2%) were incorporated to assess their performance. Twenty experiments were performed to assess the sample's deformation, von Mises stress, safety factor, stiffness, and mass. The SWR was calculated by dividing the Ultimate Load (UL) by the corresponding Applied Load (AL). The results showed a reduction of maximum deformation of 25% to 26% for 0.5 wt%, 33% to 34% for 1 wt%, and 26% to 27% for 2 wt% respectively. The findings also indicated that the samples demonstrated a 34% to 35% increase in stiffness and an 11% to 12% increase in SWR, and a 8.9% increase in mass. The unreinforced lattice showed a break in the yield stress range of 300 N to 400 N, whereas the 2 wt% loading showed a safety factor of 1.0 at 500 N. In Summary, uniform reinforcement improved the load bearing of lattices.

Keywords: *Octet-truss lattice, PLA, recycled steel fiber, ANSYS simulation, strength-to-weight ratio, additive manufacturing.*

1. INTRODUCTION

Additive manufacturing (AM) has created the field of lightweight structural design by allowing the design of lattices that eliminate much of the material normally used in a design by adding it only where it is needed [1]. The unit cell of an octet-truss lattice exhibits the all-tetrahedral strut arrangement characterized by deformation by stretching rather than bending. An 84 × 84 × 84 mm lattice made by extrusion of an axial lattice and used as a reinforcement had an ultimate compressive strength of 17.4 MPa and a modulus of elasticity of 162.8 MPa, and reduced the need for 219,520 polymer connections. compared to conventional 3D printing [2].

FDM (stereolithography) is the dominant polymer lattice manufacturing method using PLA (Polylactic acid) as the most common material because of its low price [3]. Although the quality of the unreinforced PLA is average, the best tensile strength of PLA dust-filled and fully infused using Taguchi optimized parameters has been reported at 47.84 MPa [3].

Gauss et al. [5] assert that short lyocell fiber-reinforced PLA shows the following mechanical properties: tensile strength of 85 MPa and elastic modulus of 7.2 GPa. What is more, sustainability concerns imply the use of recycled fibers as a literature review of 1,525 articles reveals that recycled fibers have more than 93% of their initial tensile strength following adequate recycling, even though physical properties undergo an essential drop due to mechanical recycling which may reduce values by up to 29%. The combination of ductility of steel materials with their low embodied costs makes it possible to elaborate effective techniques of reinforcement although this issue is not yet investigated within the framework of FDM.

The need for the joint consideration of the ideas of an FDM octet-truss lattice reinforcement using recycled steel fibres with an approach that accounts for the stress distribution in

the lattice rather than being uniformly applied. Conducting physical experiments for each combination of the above reinforcement/placement approaches would require a huge number of large-scale specimens and long experiments, but the finite element method is a good solution due to less effort when evaluating all the combinations once the geometry is determined and equivalent properties of the composite are obtained. For this purpose, ANSYS Static Structural will be used for making calculations for the CAD model of the octet-truss sample and its load testing. The mechanical behavior of the specimens produced of pure PLA, 0.5, 1, and 2 wt% of recycled steel fibre reinforced PLA produced with all three placement techniques (uniform, directional placement along the load direction and placement concerning the high-stress zones) was studied in terms of deformation, von Mises stress, safety factor, rigidity, weight and SWR.

2. LITERATURE REVIEW

2.1 Octet-Truss Lattice Mechanics

The stretch-dominated behavior derived from octet-truss cell construction provides better stiffness and strength-to-mass ratio as compared to bending-dominated geometries [2]. Bagheri et al. tested the strut radii of 0.4 to 0.6 mm (relative densities from 34.7 to 61.8%) showing that modulus and strength of material increased proportionally to the strut radius and that FEM forecasts almost corresponded with experimental findings for height-to-width ratios of 4 [6], which is highly relevant for the current FEM methodology applied in this work. Bolan, Dean, and Bardelcik reported that the energy absorption of octet-truss structure at a strain of 0.5 varied from 0.02 to 1.80 MJ/m³ depending on density and strut radius [7], thus confirming their crucial role as performance parameters. Furthermore, Poddar et al. demonstrated that polymer fibers reinforced by struts produced via axial lattice extrusion have a significantly reduced amount of polymer junctions as compared to traditional printing technologies [2].

2.2 Fiber-Reinforced Composites in Material Extrusion

Use of short and continuous fiber reinforcement of FDM polymers increases their tensile and flexural properties significantly when compared with unreinforced resin, but the benefits of this method will depend on the quality of bonding between fibers and matrix [4], [8]. Optimized lyocell-PLA composite from Gauss et al. had 85 MPa and 7.2 GPa accordingly [4]. However, unmodified formulations demonstrated low elongation but higher stiffness [4]. Wang et al. reported a 17.01% increase in tensile strength and a 21.4% increase in flexural strength for short-carbon-fiber nylon composites at 15 to 25 wt% fiber loading; nonetheless, higher loading (35 wt%) led to lower melt flow without any additional increase in mechanical properties [8].

2.3 Recycled and Metallic Fiber Reinforcement

The study conducted by Veres and Tănase analyzing 1,525 papers showed that the tensile strength of recycled fiber-reinforced polymers remains at 93% of virgin tensile strength when utilizing optimal pyrolysis recycling, while mechanical recycling brings down physical properties up to 29% [5]. O'Brien and colleagues reported that stainless-steel-fiber composites performing 144 to 288 hours of accelerated corrosion tests maintained mechanical stability and corrosion resistance against stainless sheets [9].

2.4 Lattice Design Optimization

The findings of the material of Khan and Riccio demonstrate that lattice structures in aviation are made by synchronizing the topology, density, and manufacturing constraints. The researchers discovered that the lattice structures can become graded and not uniform [1]. The results of El Khdir's research clarify that density-based optimization can be combined with homogenized models of lattice enabling the usage of local principles regulating properties of the materials based on the local stress field instead of using a single principle for the whole structure [10].

2.5 PLA Lattice Validation and FDM Process Considerations

Yahya and Pramono validated the current modeling method by combining finite element analysis with physical compression testing of the FDM-printed PLA octet-truss lattices at different quantities of unit cells and geometrical scaling factors, obtaining an FEA-to-experiment agreement of 1.70% error, as well as regression values explaining 99.7% of variations in failure load [11]. This high level of correspondence between the two methods lends support to the applicability of the current purely ANSYS method as a prediction tool prior to actual experiments being conducted. Since the efficiency of reinforcement is directly related to the quality of the process, some additional observations related to the research findings can be made: a review of the PLA FDM additives by Plamadiala et al. indicates that although fiber reinforcement increases the tensile strength and stiffness of materials, in some cases, the introduction of solid fillers leads to agglomeration of the material at high concentrations, directly following the observed non-monotonous nature of the failures of materials [12]. Lanzotti et al. claimed that the thickness of the layers, the orientation of the fill and the number of shells above influence the tensile strength and elongation at break of PLA regardless of its composition [13]. In contrast, Maguluri et al. argued that the material temperature has the strongest influence on tensile properties of PLA, surpassing the effects of fill density or

printing speed [14]. In their extensive review of the FDM process and the materials and application that employ such processes Rajan et al. mentioned the discussed factors as the main ones affecting mechanical characteristics of the whole range of materials [15]. These results imply that in any future investigation of the reinforced lattice in this work, some criteria have to be fixed so that the differences between the values can be attributed to the differences in the content of steel fibers.

3. METHODOLOGY

A single lattice structure stored in a CAD STEP file was kept the same during twenty runs of ANSYS Static Structural simulations (five loads × four materials), making it unnecessary to have a specimen for every combination. All information in Section 4 was taken directly from the ANSYS report that has been printed for each run.

3.1 CAD Model, Mesh, and Boundary Conditions

The octet-truss test piece was acquired as one solid piece (Figure 1) with a bounding box size of 40 × 40 × 40 mm, a volume of 7217.9 mm³ and mass of 8.9501 g (without reinforcement). As the entire structure was a single, continuous solid, there was no need for the definition of bonded contact at junctions of the struts. The base side was restrained in all degrees of freedom, and a load in the form of compressive force (in the Y-direction only, as confirmed by the data on the reaction force) was applied to the upper side at five values — 100, 200, 300, 400, and 500 N — for each of the four types of material with the ramping within one load step, with large geometry non-linearity taken into account and with the use of direct solver. In ANSYS Mechanical, the mesh patch-conforming tetrahedron mesh (20 mm specified element size, medium sizing) was generated consisting of 111,497 nodes and 42,523 elements, and this mesh is the same in all twenty trials.

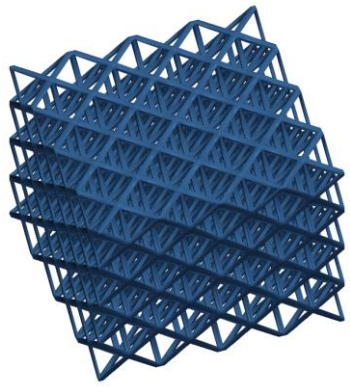


Figure 1. Isometric CAD rendering of the octet-truss lattice specimen (40 × 40 × 40 mm).

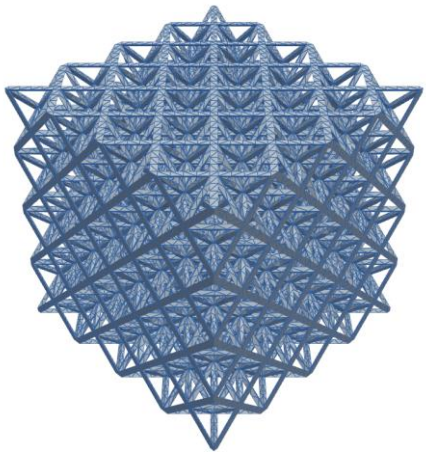


Figure 2. Finite element mesh generated in ANSYS Mechanical (111,497 nodes, 42,523 elements).

3.2 Material Properties

Modeling recycled steel fibers discretely in every strut would violate the conditions of the academic license; thus, composite materials are represented using average isotropic properties assigned in the ANSYS Engineering Data as listed in Table 1 and taken directly from the Material Data sections of the related reports. All materials were assumed to be elastic and isotropic.

Property	PLA (0%)	PLA + 0.5% SF	PLA + 1% SF	PLA + 2% SF
Density (kg/m³)	1240	1268	1295	1350
Young's Modulus (GPa)	3.20	3.45	3.75	4.35
Poisson's Ratio	0.36	0.35	0.35	0.34
Tensile Yield Strength (MPa)	55	58	62	68
Tensile Ultimate Strength (MPa)	60	64	69	76

Table 1. Homogenized material properties assigned to each configuration (ANSYS Engineering Data).

3.3 Reinforcement Strategy and Evaluation Metrics

Results reported here cover the uniform strategy (entire specimen modeled in one material) across the full load range, giving the 20-run matrix in Table 3. Directional and high-stress-zone strategies (Section 1) remain for the next stage. For each run, total deformation, equivalent (von Mises) stress, equivalent elastic strain, and Stress-Tool factor of safety (max-equivalent-stress theory vs. tensile yield) were read as minimum/maximum/average values. Stiffness was derived as $k = F/\delta max$, and strength-to-weight ratio (SWR) as $(F \times FOSmin) /$ mass. The reports do not include a separate maximum-principal-stress result, so von Mises stress and FOS serve as the primary strength indicators below.

4. RESULTS AND DISCUSSION

Table 3 summarizes mass, peak deformation, peak von Mises stress, minimum FOS, stiffness, and SWR for all twenty runs. One data-quality issue was found: the 500 N / 0.5 wt% SF report duplicates the 400 N solution (identical results; internal load recorded as −400 N), so this configuration was evidently not re-solved at 500 N. It is marked with an asterisk in Table 3, excluded from Figure 4's trend lines, and should be re-run before the study is finalized.

Table 3. ANSYS results across all five compressive loads and four materials. *500 N/0.5 wt% SF report duplicates the 400 N solution; excluded from trends

Load (N)	Material	Mass (g)	Max Deform. (mm)	Von Mises (MPa)	Min FOS	Stiffness (N/mm)	SWR (N/g)
100	PLA (0%)	8.950	0.0765	15.25	3.61	1306.9	40.31
100	0.5 wt% SF	9.152	0.0712	15.39	3.77	1404.1	41.19
100	1 wt% SF	9.347	0.0655	15.39	4.03	1525.7	43.09
100	2 wt% SF	9.744	0.0567	15.53	4.38	1763.8	44.94
200	PLA (0%)	8.950	0.1523	30.35	1.81	1313.0	40.50
200	0.5 wt% SF	9.152	0.1418	30.64	1.89	1410.2	41.37
200	1 wt% SF	9.347	0.1306	30.66	2.02	1531.9	43.27
200	2 wt% SF	9.744	0.1130	30.95	2.20	1770.1	45.10
300	PLA (0%)	8.950	0.2275	45.30	1.21	1319.0	40.70
300	0.5 wt% SF	9.152	0.2118	45.74	1.27	1416.4	41.56
300	1 wt% SF	9.347	0.1951	45.79	1.35	1538.0	43.45
300	2 wt% SF	9.744	0.1689	46.25	1.47	1776.2	45.26
400	PLA (0%)	8.950	0.3019	60.11	0.91	1325.1	40.89
400	0.5 wt% SF	9.152	0.2812	60.73	0.96	1422.5	41.74
400	1 wt% SF	9.347	0.2591	60.82	1.02	1544.0	43.62
400	2 wt% SF	9.744	0.2244	61.43	1.11	1782.3	45.44
500	PLA (0%)	8.950	0.3756	74.74	0.74	1331.1	41.11
500	0.5 wt% SF*	9.152	—	—	—	—	—
500	1 wt% SF	9.347	0.3226	75.68	0.82	1550.1	43.82
500	2 wt% SF	9.744	0.2796	76.53	0.89	1788.5	45.59

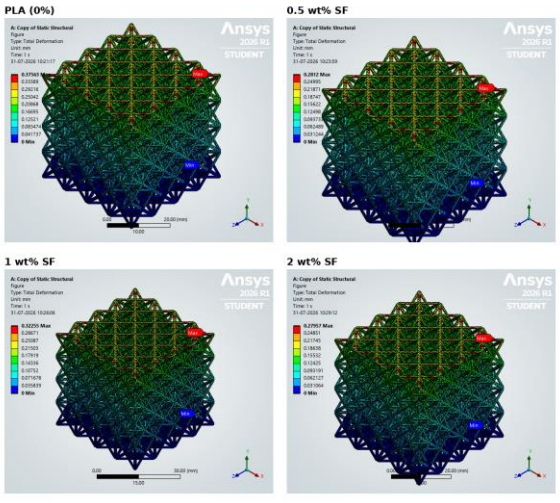


Figure 3. Total deformation contours at 500 N compression for all four materials (ANSYS Mechanical exports).

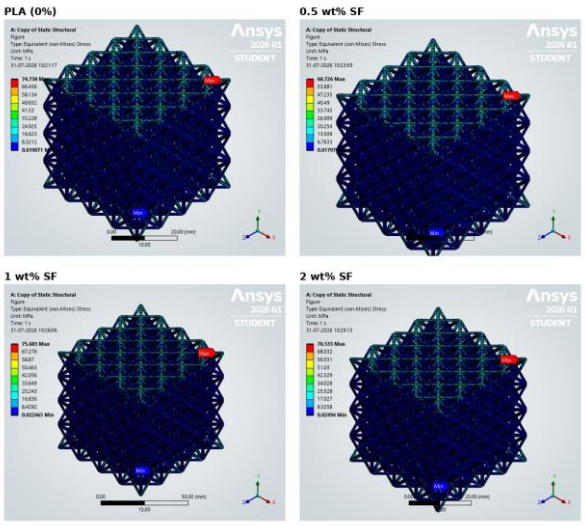


Figure 4. Equivalent (von Mises) stress contours at 500 N compression for all four materials.

Deformation and stress scale approximately linearly with load for every material, as expected in this linear-elastic regime (Figure 5), while the absolute gap between materials widens with load: pure PLA and 2 wt% SF differ by 0.020 mm at 100 N but 0.096 mm at 500 N, even though the percentage reduction (~26%) stays roughly constant. Stiffness rises consistently with reinforcement at every load — from ~1307–1331 N/mm (PLA) to ~1764–1789 N/mm (2 wt% SF), a ~34–35% gain that closely tracks the 35.9% increase in assigned modulus (3.20 to 4.35 GPa), confirming the homogenized material assignment behaves consistently with basic mechanics of materials.

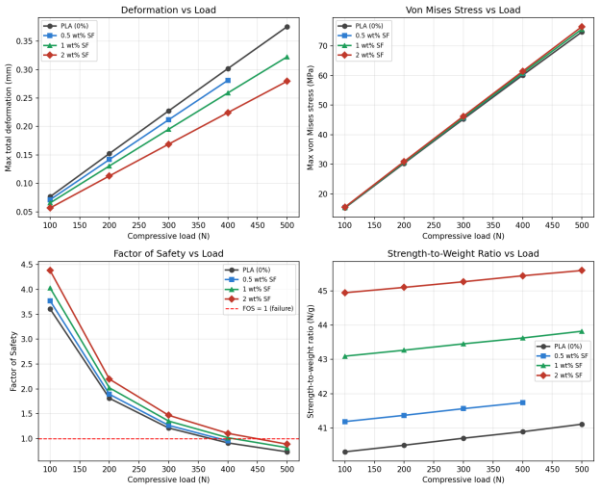


Figure 5. Deformation, von Mises stress, factor of safety, and strength-to-weight ratio vs. applied load for each material (0.5 wt% SF/500 N omitted).

The most important trend is factor of safety (Figure 5, bottom-left): pure PLA crosses FOS = 1 between 300 N (1.21) and 400 N (0.91), meaning local yielding is predicted in that range. Reinforcement delays but does not eliminate this: 1 wt% SF crosses FOS = 1 between 300–400 N (1.35→1.02), and even 2 wt% SF, still above threshold at 400 N (1.11), drops to 0.89 by 500 N. Table 3 shows every material comfortably above FOS = 3.6 at 100 N alone — underscoring why the full load range, not a single load case, is needed before drawing conclusions about usable load.

SWR rises modestly but consistently with reinforcement at every load — e.g., 40.31 to 44.94 N/g at 100 N, and 41.11 to 45.59 N/g at 500 N (excluding the flawed 0.5 wt% SF/500 N entry) — roughly 11–12% regardless of load, for only an 8.9% mass increase (8.950 to 9.744 g). Since this gain is essentially load-independent, the key design question is less which load to reinforce for and more whether 2 wt% SF alone keeps the lattice above FOS = 1 at its intended service load — which, per Table 3, holds only up to roughly 350–400 N for this geometry. This motivates the directional and high-stress-zone strategies from Section 2.4 [1], [10]: concentrating steel fiber in the highest-stress struts may raise the failure load more effectively than uniform 2 wt% reinforcement alone, for a similar mass penalty.

5. CONCLUSION

This study evaluated recycled steel-fiber reinforcement of an FDM-printed PLA octet-truss lattice using ANSYS Static Structural on a CAD-modeled 40 mm specimen (111,497 nodes, 42,523 elements) across five compressive loads (100–500 N) and four materials. Increasing steel-fiber content from 0% to 2 wt% consistently reduced peak deformation by ~25–26%, increased stiffness by ~34–35%, and increased SWR by 11–12%, for an 8.9% mass increase. Critically, the unreinforced lattice is predicted to yield locally between 300 N and 400 N, and even 2 wt% SF drops below FOS = 1 by 500 N — so uniform reinforcement alone extends, but does not remove, the load ceiling within the tested range. The literature reviewed suggests spatially selective reinforcement may raise this threshold further without the full mass penalty of uniform reinforcement [1], [10]; testing this, and re-running the flawed 500 N/0.5 wt% SF case, are the immediate next steps.

6. FUTURE SCOPE

Priorities are: (1) re-solving the 500 N/0.5 wt% SF case; (2) running the directional and high-stress-zone reinforcement strategies across the same load range, to test whether they raise the FOS = 1 threshold above 500 N without the full mass penalty of uniform 2 wt% reinforcement; and (3) locating the precise load at which each material first drops below FOS = 1 via intermediate load steps (300–400 N; 400–500 N for 2 wt% SF). Longer-term work includes physical validation of the best-performing configuration, refining material estimates from measured filament properties, and formal topology optimization of reinforcement placement.

REFERENCES

[1] Khan, Numan, and Aniello Riccio. "A systematic review of design for additive manufacturing of aerospace lattice structures: Current trends and future directions." Progress in Aerospace Sciences 149 (2024): 101021.

[2] Poddar, Pritam, Mark Olles, and Denis Cormier. "Mechanical response of carbon composite octet truss structures produced via axial lattice extrusion." Polymers 14.17 (2022): 3553.

[3] Ekşi, Seçil, and Cetin Karakaya. "Effects of process parameters on tensile properties of 3D-printed PLA parts fabricated with the FDM method." Polymers 17.14 (2025): 1934.

[4] Gauss, Christian, et al. "3D-printed polylactide composites reinforced with short lyocell fibres–Enhanced mechanical properties based on bio-inspired fibre fibrillation and post-print annealing." Additive Manufacturing 77 (2023): 103806.

[5] Veres, Cristina, and Maria Tănase. "A bibliometric and systematic review of the use of recycled composite materials with an emphasis on the mechanical performance of structures." Materials 18.3 (2025): 607.

[6] Bagheri, Ali, et al. "Determination of the elasticity modulus of 3D-printed octet-truss structures for use in porous prosthesis implants." Materials 11.12 (2018): 2420.

[7] Bolan, Matthew, Mackenzie Dean, and Alexander Bardelcik. "The energy absorption behavior of 3D-printed polymeric octet-truss lattice structures of varying strut length and radius." Polymers 15.3 (2023): 713.

[8] Wang, Yesong, et al. "Effect of fiber content on the preparation and mechanical properties of 3D printed short carbon fiber reinforced PA composites." Polymers 17.5 (2025): 671.

[9] O'Brien, Caitlin, et al. "Mechanical behavior of stainless steel fiber-reinforced composites exposed to accelerated corrosion." Materials 10.7 (2017): 772.

[10]El Khadiri, Issam, et al. "Topology optimization methods for additive manufacturing: a review." International journal for simulation and multidisciplinary design optimization 14 (2023): 12.

[11] Yahya, Muhammad Yusri Dzal, and Agus Sigit Pramono. "Numerical and experimental investigation of scaling laws in PLA octet-truss lattice structures under compression load." Jurnal Polimesin 23.6 (2025): 779-789.

[12] Plamadiala, Ioan, et al. "Enhancing polylactic acid (PLA) performance: A review of additives in fused deposition modelling (FDM) filaments." Polymers 17.2 (2025): 191.

[13] Lanzotti, Antonio, et al. "The impact of process parameters on mechanical properties of parts fabricated in PLA with an open-source 3-D printer." Rapid Prototyping Journal 21.5 (2015): 604-617.

[14] Maguluri, Nagarjuna, Gamini Suresh, and K. Venkata Rao. "Assessing the effect of FDM processing parameters on mechanical properties of PLA parts using Taguchi method." Journal of Thermoplastic Composite Materials 36.4 (2023): 1472-1488.

[15] Rajan, Kumaresan, et al. "Fused deposition modeling: process, materials, parameters, properties, and applications." The International Journal of Advanced Manufacturing Technology 120.3 (2022): 1531-1570.